



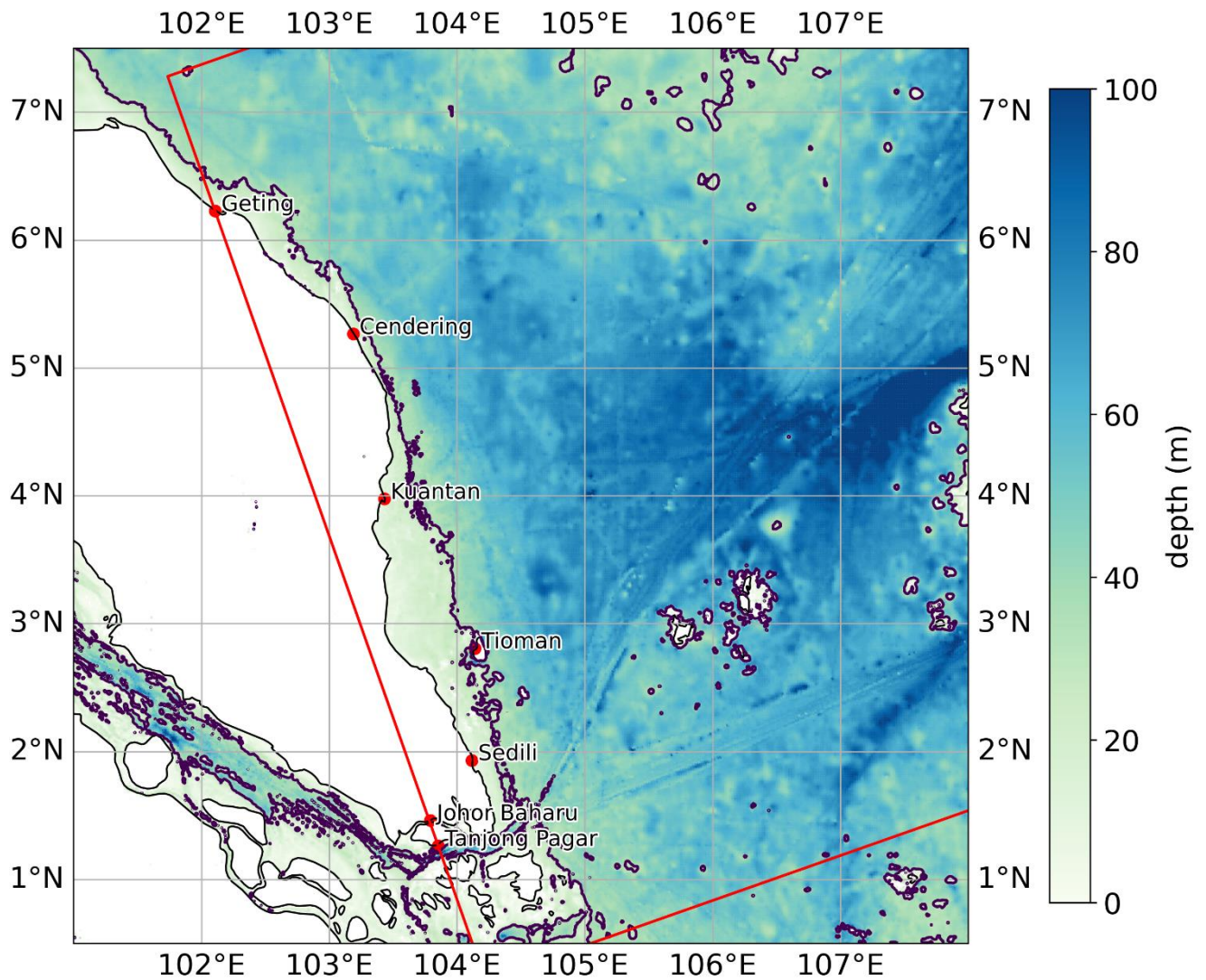
*Supplement of*

## **Tide–surge interaction observed at Singapore and the east coast of Peninsular Malaysia using a semi-empirical model**

**Zhi Yang Koh et al.**

*Correspondence to:* Zhi Yang Koh (kohz0034@e.ntu.edu.sg)

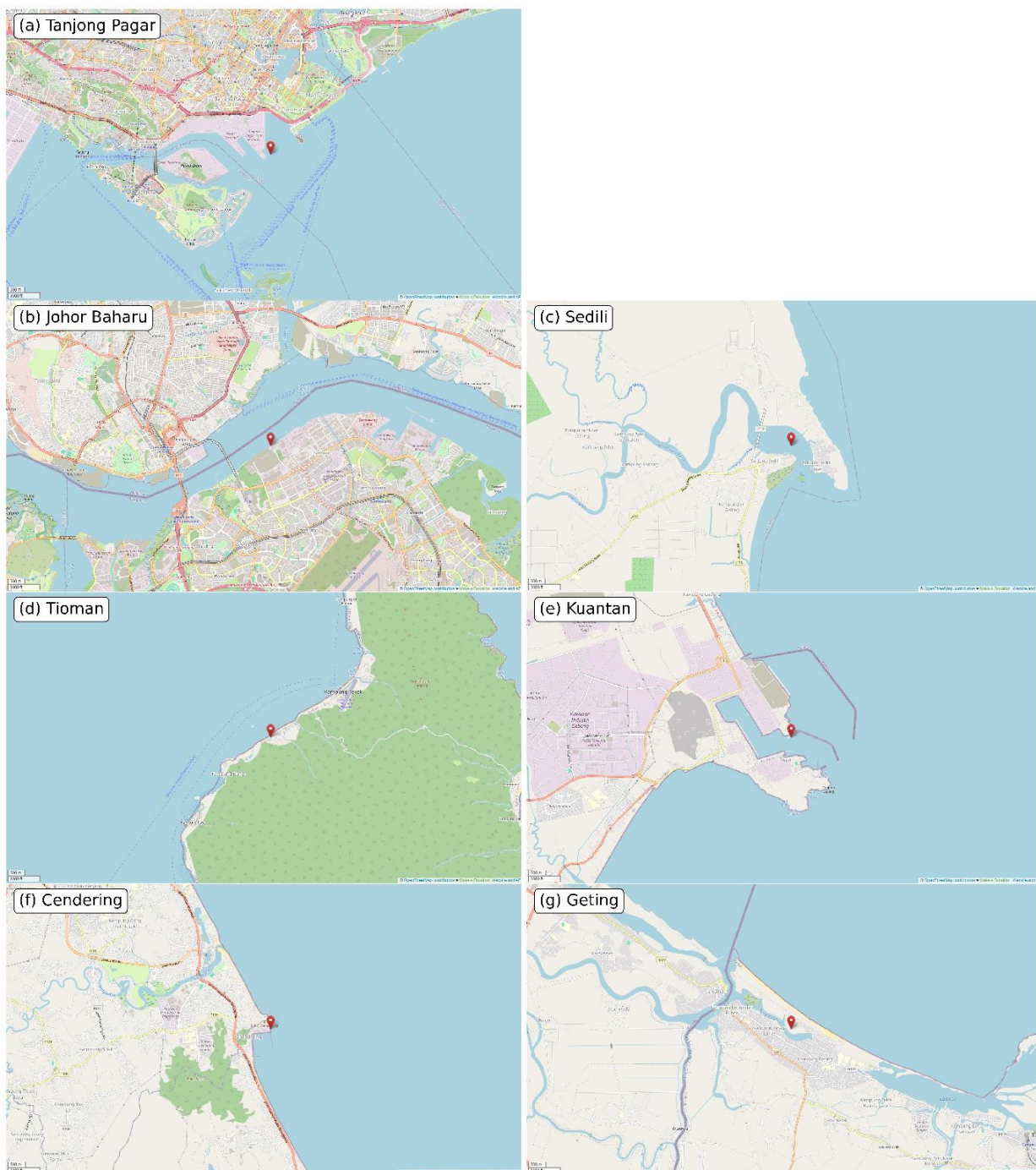
The copyright of individual parts of the supplement might differ from the article licence.



13  
 14 **Figure S1: Bathymetry (in m) near the seven tide gauges, obtained from GEBCO, the General Bathymetric Chart of the Oceans**  
 15 **(GEBCO Compilation Group, 2023). The seven tide gauge stations are marked in red circles. The red rectangle denotes the region**  
 16 **where 10 m winds and mean sea level pressure are considered when calculating  $R_{\text{surge}}$  (Sect. 3.4). Contour lines at a depth of 30 m**  
 17 **are drawn in purple, beyond which we find a relatively steep descend.**

18

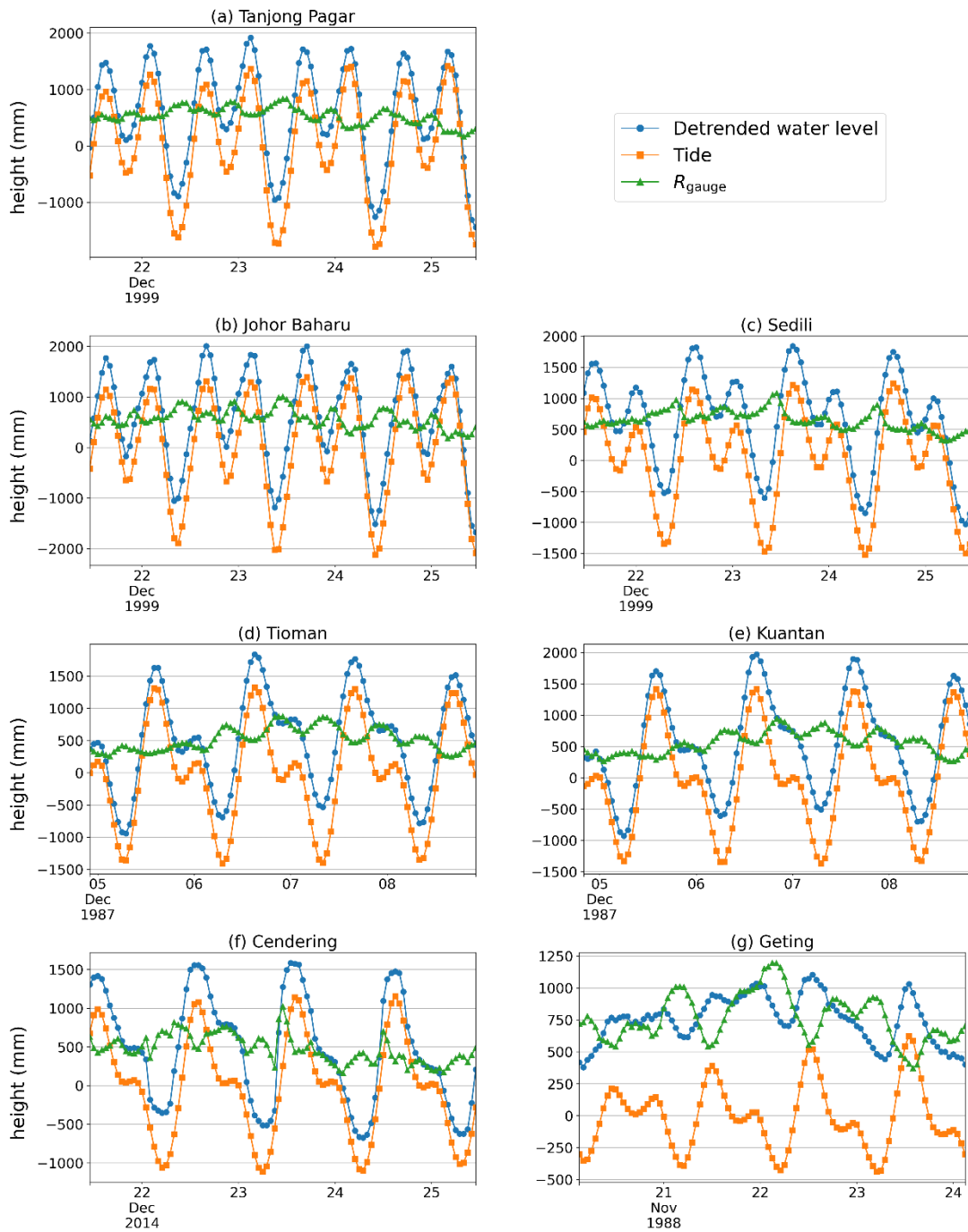
## Local characteristics around tide gauge



19  
20 **Figure S2: Local characteristics near the seven tide gauges (OpenStreetMap contributors, 2017; Caldwell et al., 2001). ©**  
21 **OpenStreetMap contributors 2017. Distributed under the Open Data Commons Open Database License (ODbL) v1.0.**

22

Timeseries during largest recorded  $R_{\text{gauge}}$

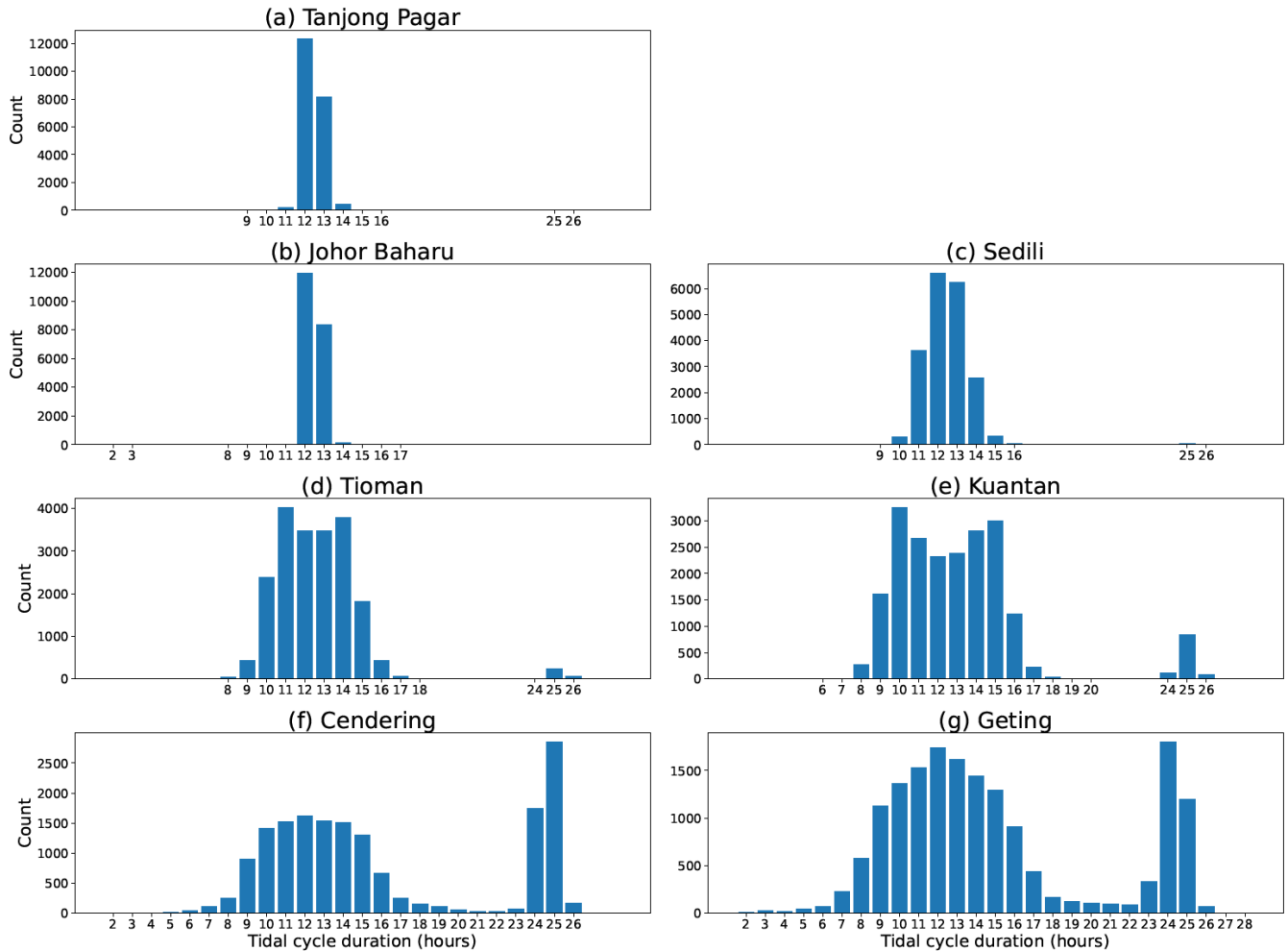


23  
24

Figure S3: Timeseries at each tide gauge location two days before and after the largest observed non-tidal residual,  $R_{\text{gauge}}$ .

25

## Distribution of tidal cycle duration



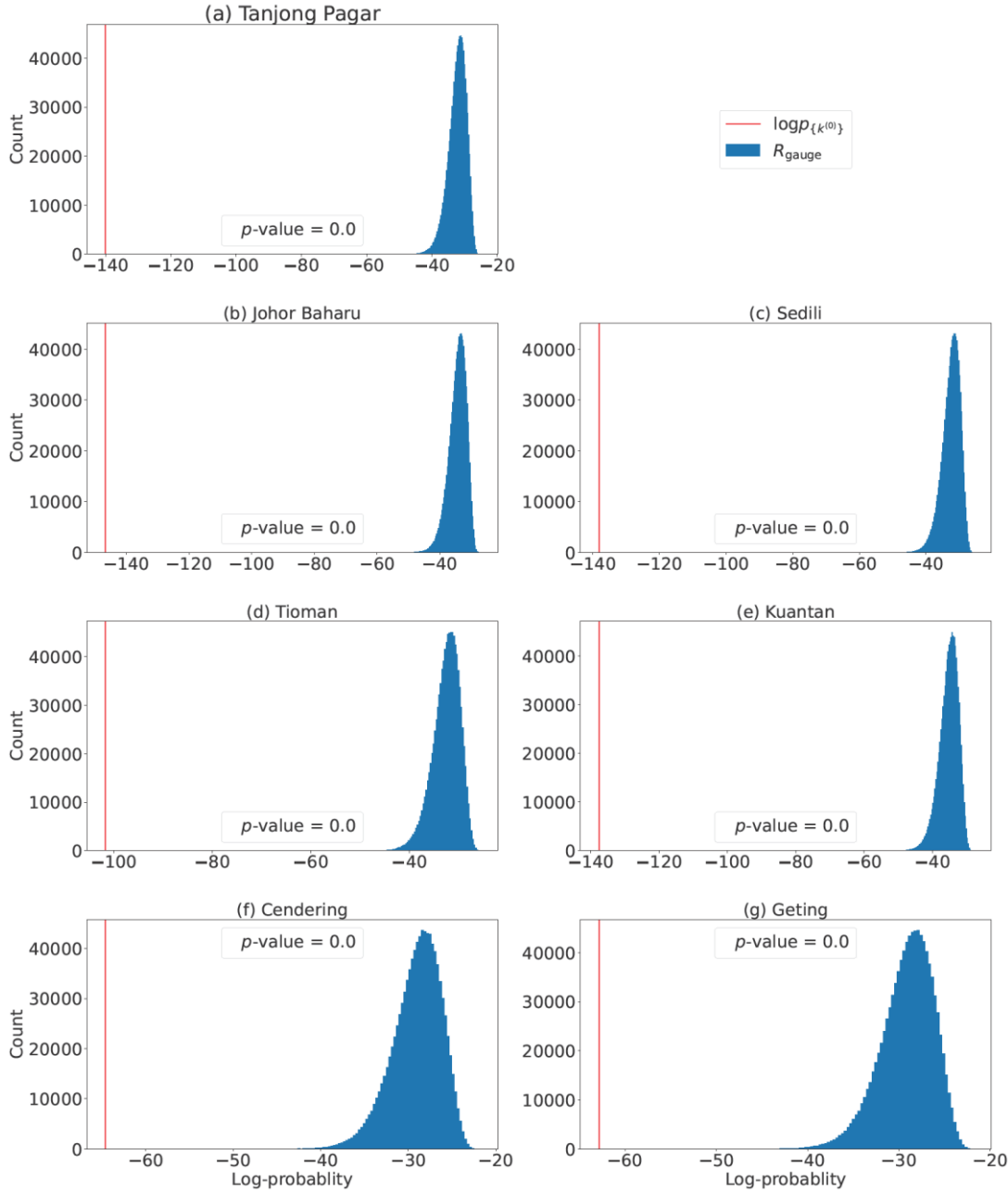
27

28 **Figure S4: Histogram of the duration of tidal cycles at each tide gauge location. Tidal cycles are defined as the duration from one**  
 29 **local minima in the hourly tidal level to the observation immediately preceding the next local minima (Sect. 3.2). Tidal cycles at**  
 30 **Tanjung Pagar and Johor Baharu are often 12–13 hours long, while the tidal cycles at the other locations are less consistent.**

31



Distribution of bootstrap sample log-probability

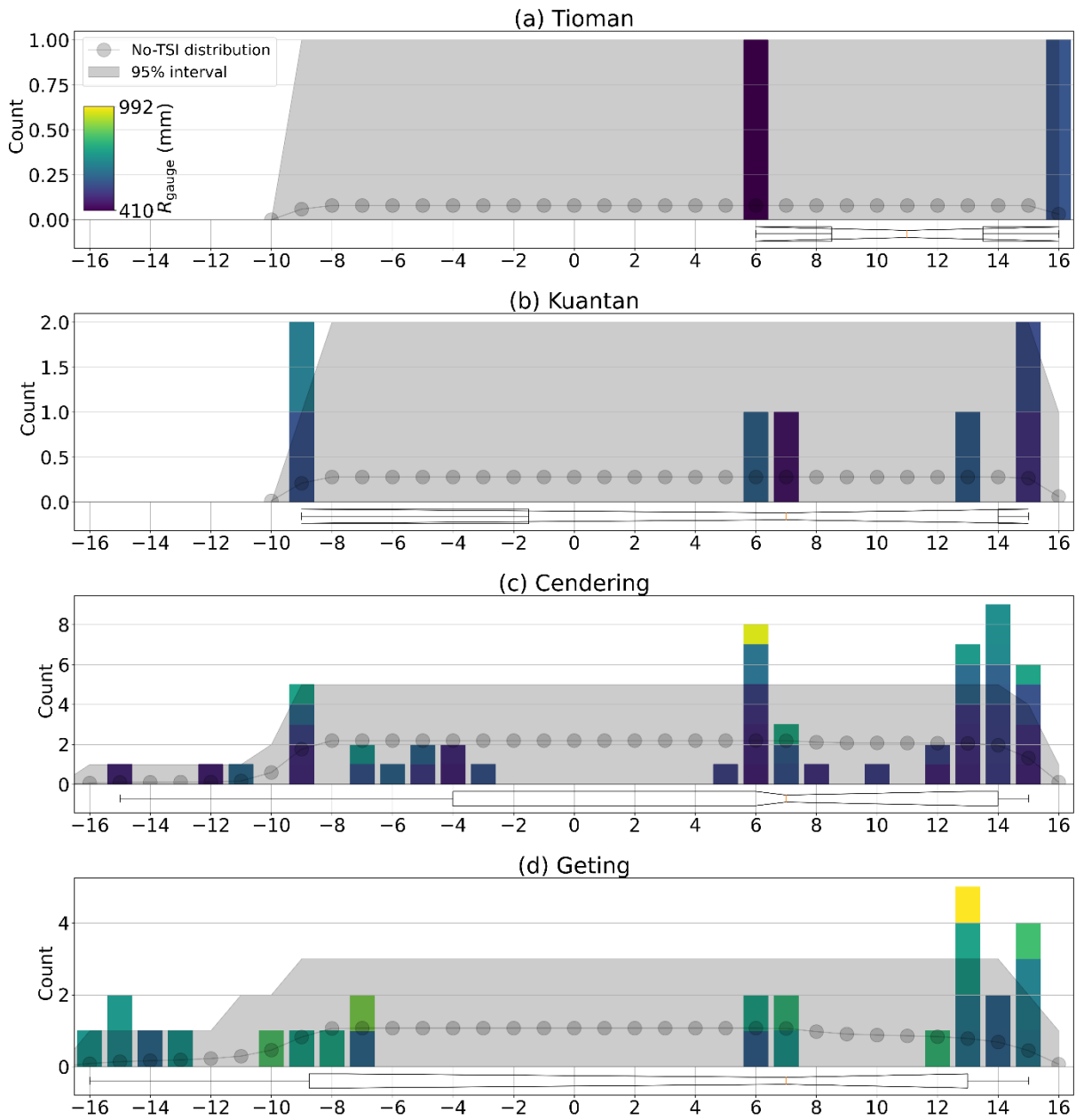


32

33 **Figure S5: Histogram of 1,000,000 log-probabilities of obtaining a randomly generated bootstrap sample from the normalized No-**  
 34 **TSI distribution  $p_h$  of  $R_{\text{gauge}}$  during semidiurnal tidal cycles. Red vertical lines indicate  $\log p_{\{k^{(0)}\}}$ , the log-probabilities of obtaining**  
 35 **the frequency distribution  $k^{(0)}$  from  $p_h$ .  $p$ -values are obtained by taking the quantile of the  $\log p_{\{k^{(0)}\}}$  within the 1,000,000 log-**  
 36 **probabilities of bootstrap samples.**

37

Number of  $R_{\text{gauge}}$  extremes found at x hours from nearest tidal high water

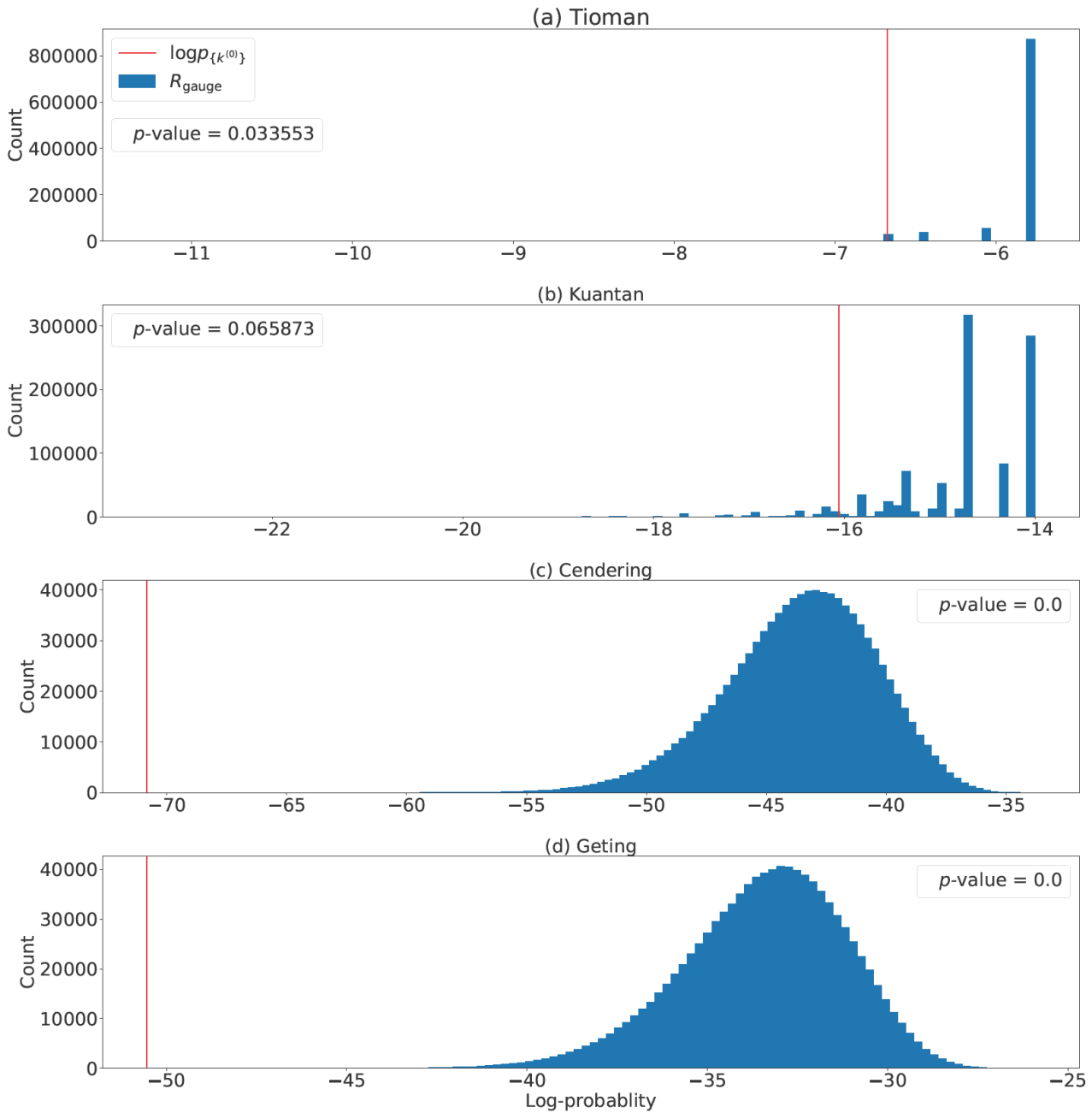


38

39 **Figure S6: The frequency distribution for extreme values of  $R_{\text{gauge}}$  and the No-TSI distribution during diurnal tidal cycles,**  
 40 **truncated at  $\pm 16$  hours from tidal high water. The frequency distribution is compared to the No-TSI distribution to determine the**  
 41 **presence of tide-surge interaction. Summary statistics of the frequency distribution are shown using the horizontal notched box plot,**  
 42 **where orange lines indicate the medians, notches indicate the 95% confidence interval of the medians, notched rectangles indicate**  
 43 **the interquartile range (IQR), whiskers indicate a range that extends up to  $1.5 \times \text{IQR}$  from the limits of the IQR, and black circles (if**  
 44 **present) indicate outliers outside this range.**

45

Distribution of bootstrap sample log-probability



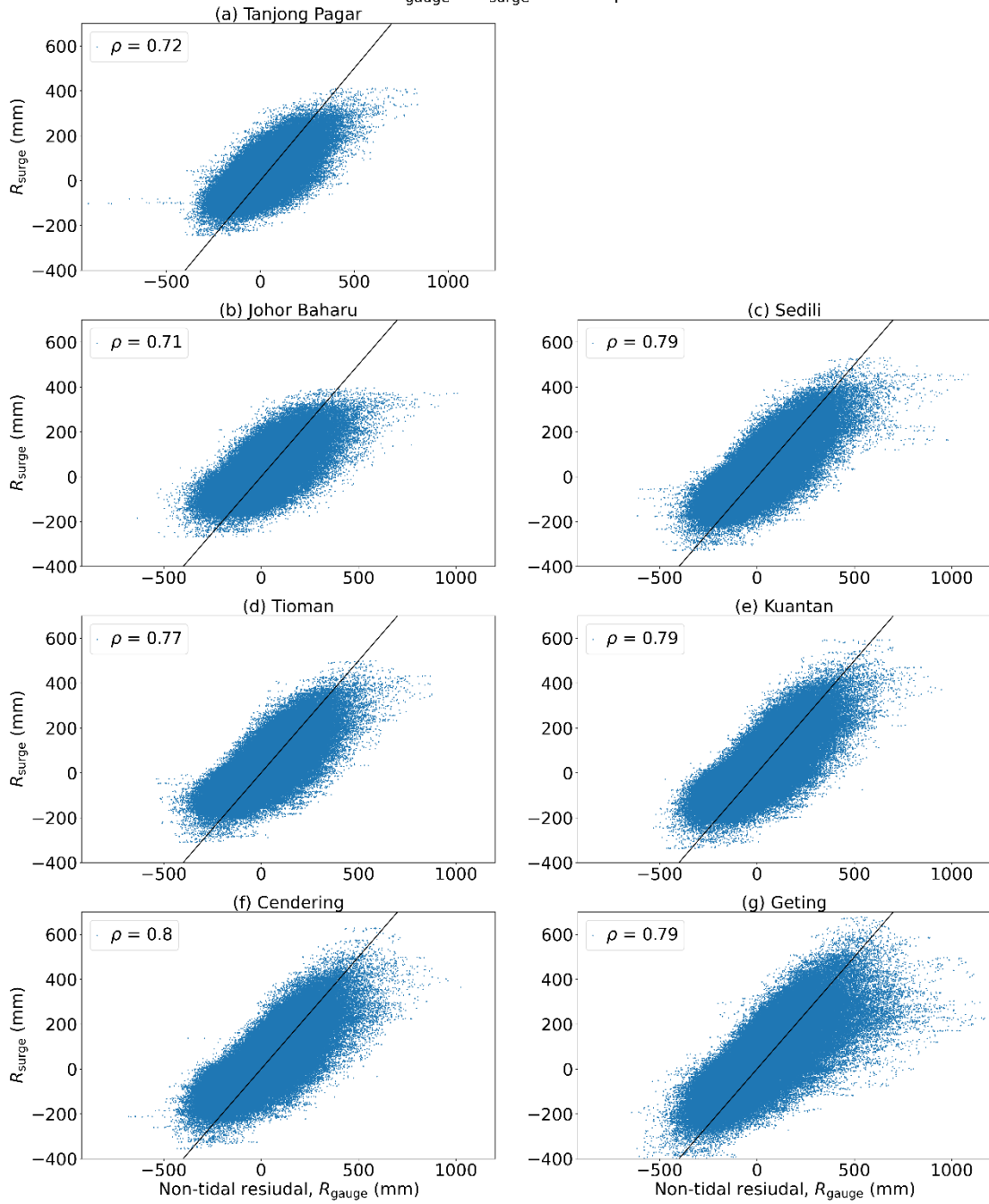
46

47 **Figure S7: Histogram of 1,000,000 log-probabilities of obtaining a randomly generated bootstrap sample from the normalized No-**  
 48 **TSI distribution  $p_h$  of  $R_{\text{gauge}}$  during diurnal tidal cycles. Red vertical lines indicate  $\log p_{\{k^{(0)}\}}$ , the log-probabilities of obtaining the**  
 49 **frequency distribution  $k^{(0)}$  from  $p_h$ .  $p$ -values are obtained by taking the quantile of the  $\log p_{\{k^{(0)}\}}$  within the 1,000,000 log-**  
 50 **probabilities of bootstrap samples.**

51



$R_{\text{gauge}} - R_{\text{surge}}$  scatter plot

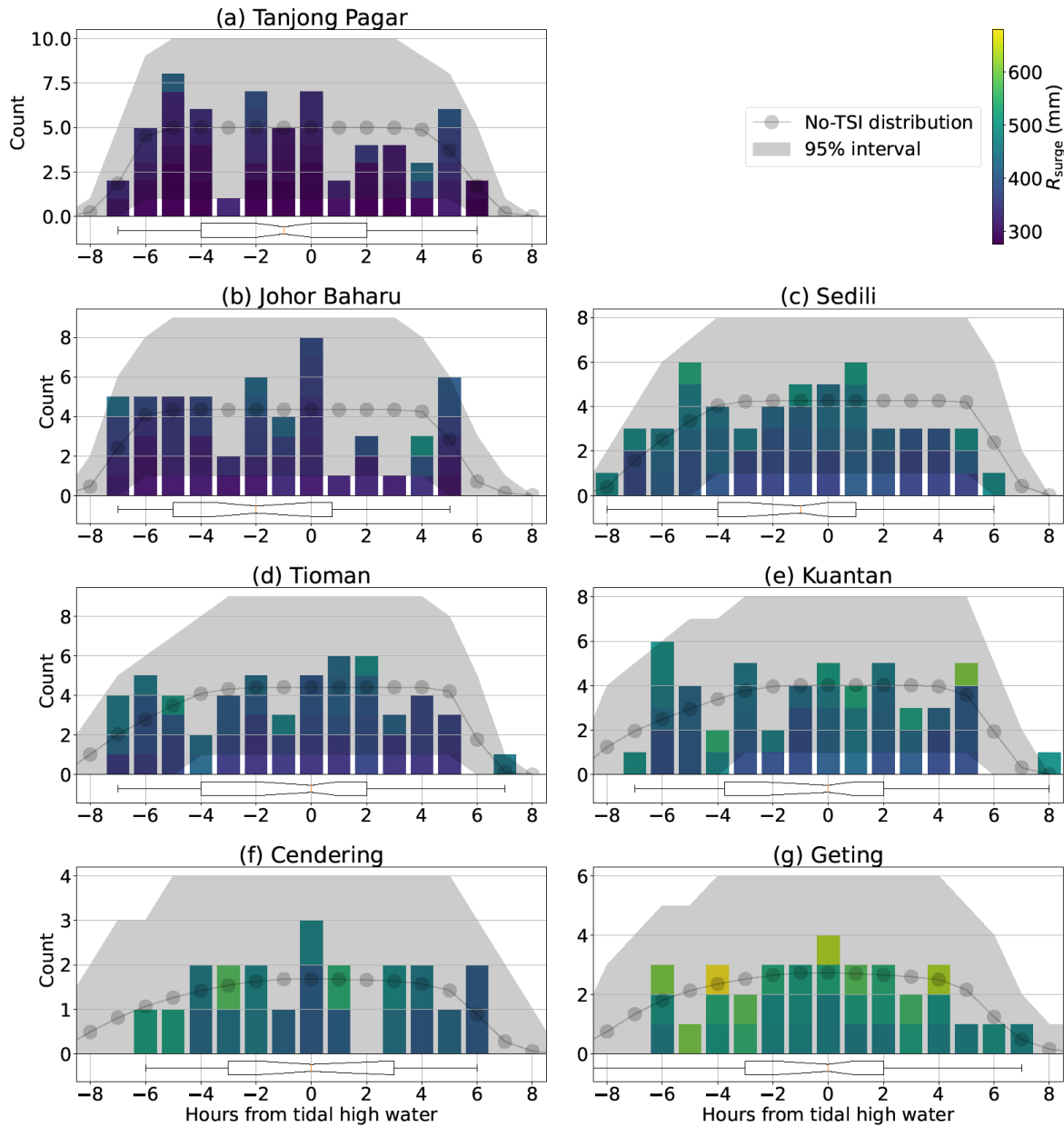


52

53 **Figure S8: Scatter plots between non-tidal residuals,  $R_{\text{gauge}}$  and  $R_{\text{wind}}$  at each tide-gauge location. The correlation coefficients of**  
54 **0.7–0.8 corresponds to a coefficient of determination of 0.5–0.6.**

55

Number of  $R_{\text{surge}}$  extremes found at  $x$  hours from nearest tidal high water

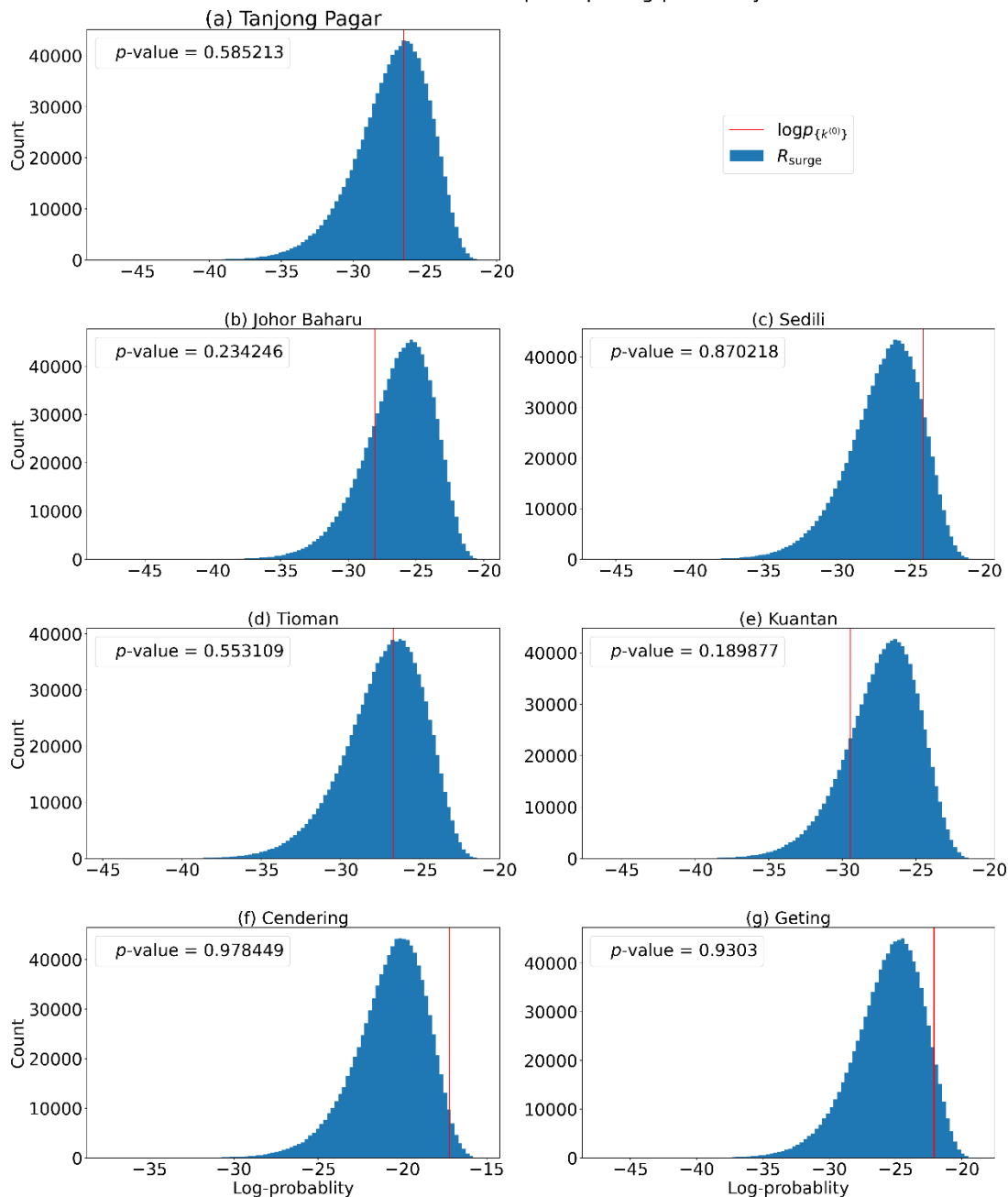


56

57 **Figure S9: The frequency distribution for extreme values of  $R_{\text{wind}}$  and the No-TSI distribution during semidiurnal tidal cycles,**  
 58 **truncated at  $\pm 8$  hours from tidal high water. The frequency distribution is compared to the No-TSI distribution to determine the**  
 59 **presence of tide-surge interaction. Summary statistics of the frequency distribution are shown using the horizontal notched box plot,**  
 60 **where orange lines indicate the medians, notches indicate the 95% confidence interval of the medians, notched rectangles indicate**  
 61 **the interquartile range (IQR), whiskers indicate a range that extends up to  $1.5 \times \text{IQR}$  from the limits of the IQR, and black circles (if**  
 62 **present) indicate outliers outside this range.**

63

Distribution of bootstrap sample log-probability

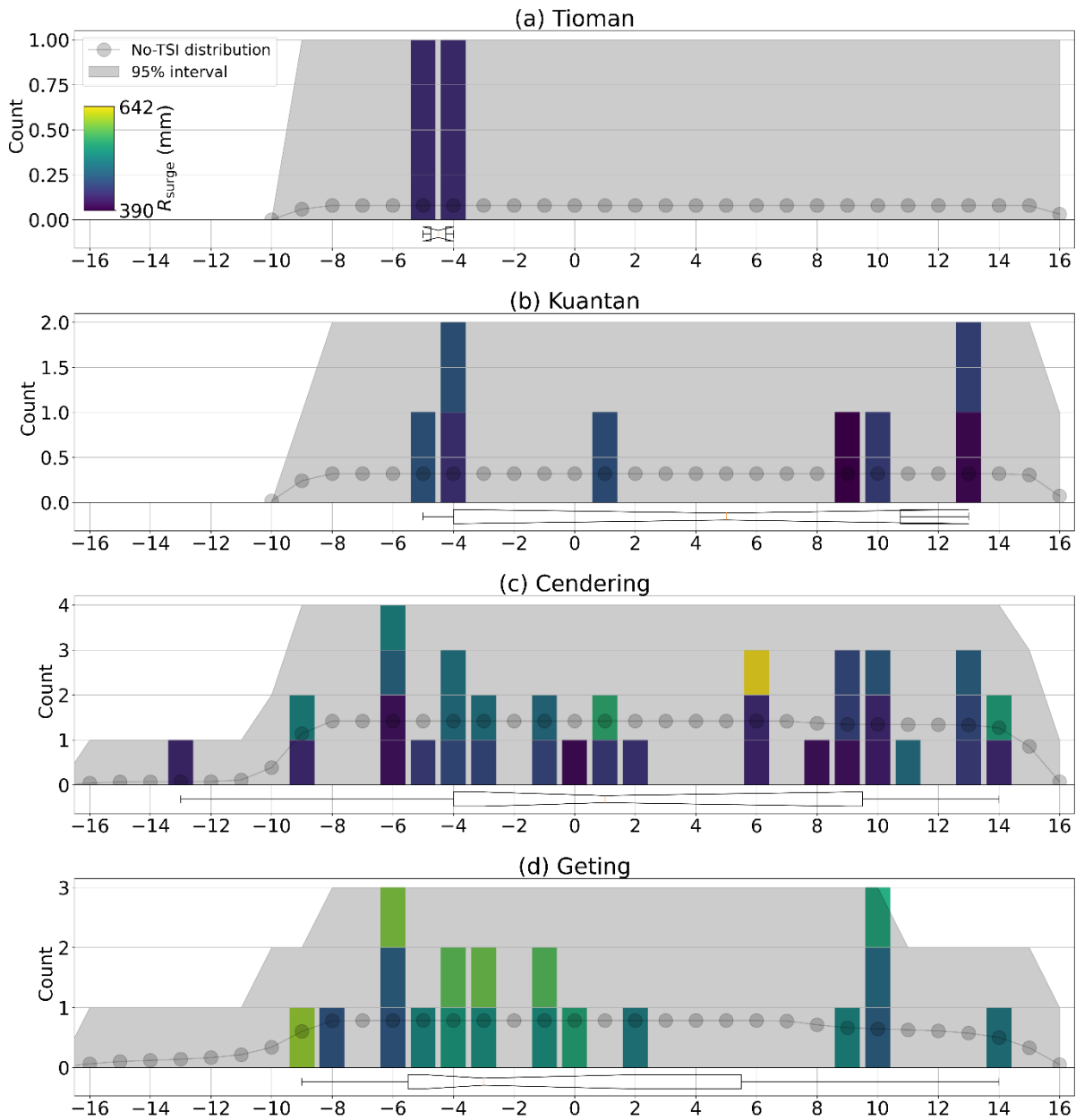


64

65 **Figure S10: Histogram of 1,000,000 log-probabilities of obtaining a randomly generated bootstrap sample from the normalized No-**  
 66 **TSI distribution  $p_h$  of  $R_{\text{wind}}$  during semidiurnal tidal cycles. Red vertical lines indicate  $\log p_{\{k^{(0)}\}}$ , the log-probabilities of obtaining**  
 67 **the frequency distribution  $k^{(0)}$  from  $p_h$ .  $p$ -values are obtained by taking the quantile of the  $\log p_{\{k^{(0)}\}}$  within the 1,000,000 log-**  
 68 **probabilities of bootstrap samples.**

69

Number of  $R_{\text{surge}}$  extremes found at x hours from nearest tidal high water

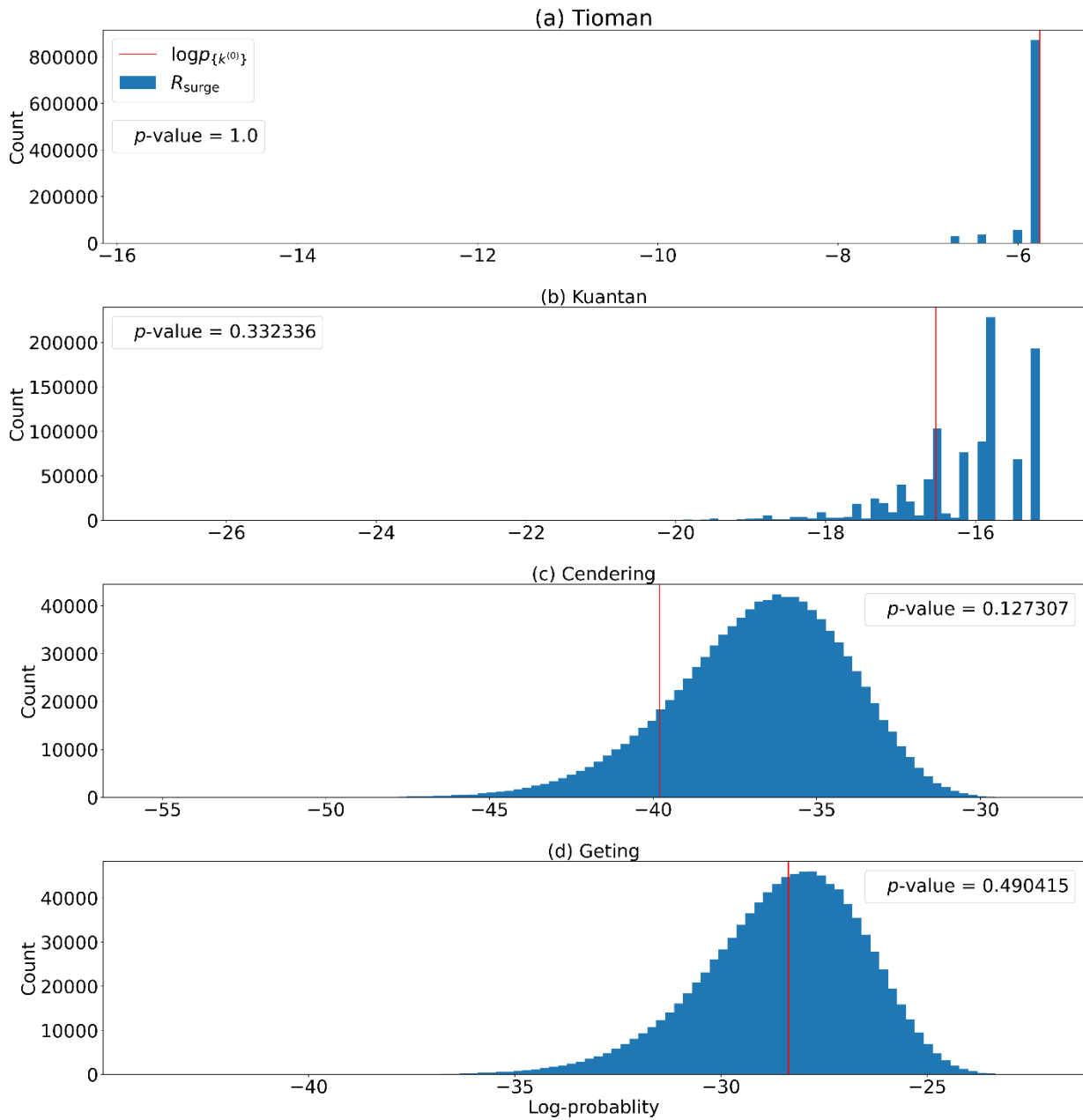


70

71 **Figure S11: The frequency distribution for extreme values of  $R_{\text{wind}}$  and the No-TSI distribution during diurnal tidal cycles,**  
 72 **truncated at  $\pm 16$  hours from tidal high water. The frequency distribution is compared to the No-TSI distribution to determine the**  
 73 **presence of tide-surge interaction. Summary statistics of the frequency distribution are shown using the horizontal notched box plot,**  
 74 **where orange lines indicate the medians, notches indicate the 95% confidence interval of the medians, notched rectangles indicate**  
 75 **the interquartile range (IQR), whiskers indicate a range that extends up to  $1.5 \times \text{IQR}$  from the limits of the IQR, and black circles (if**  
 76 **present) indicate outliers outside this range.**

77

Distribution of bootstrap sample log-probability

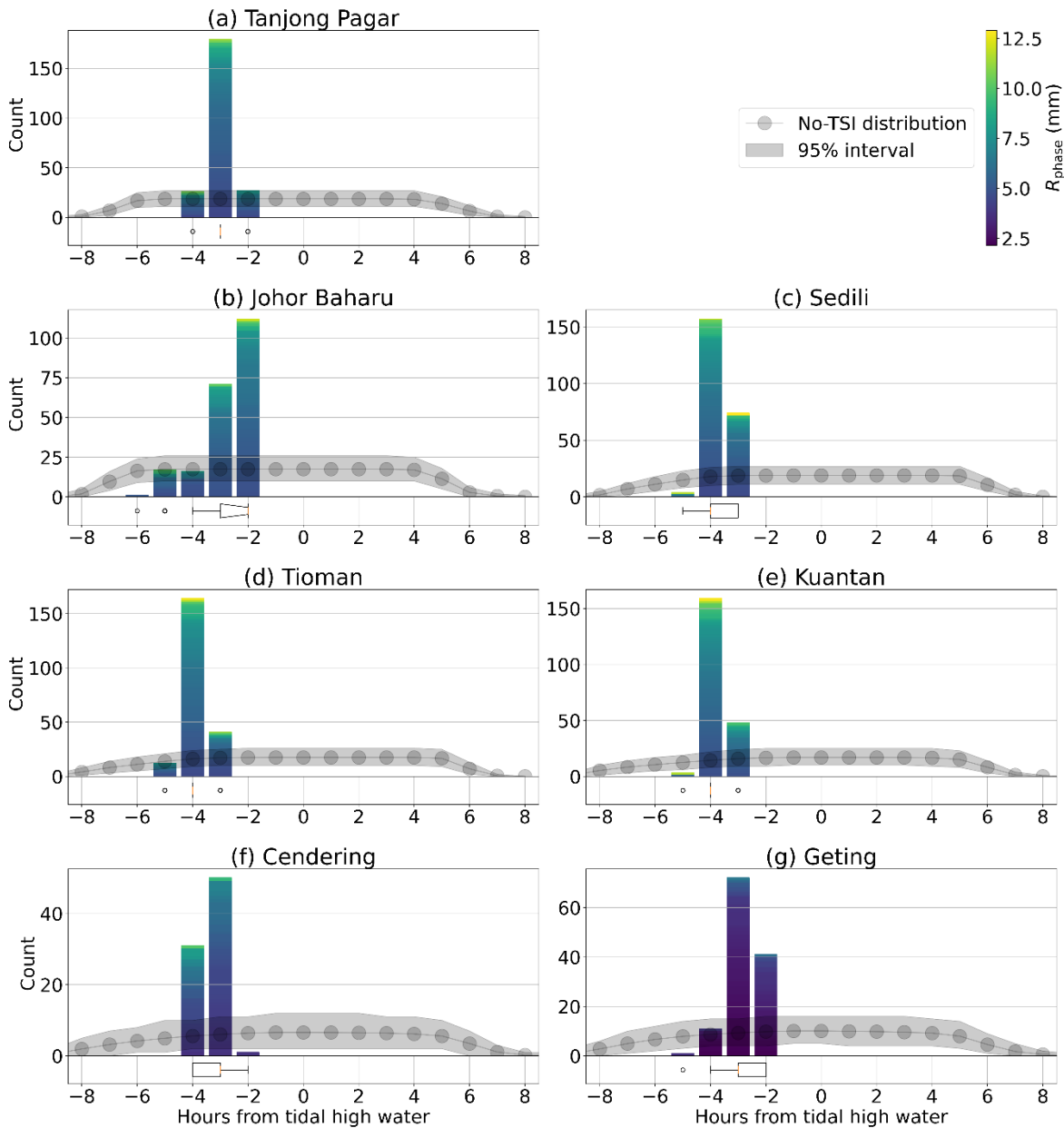


78

79 **Figure S12: Histogram of 1,000,000 log-probabilities of obtaining a randomly generated bootstrap**  
 80 **NTSI distribution  $p_h$  of  $R_{\text{wind}}$  during diurnal tidal cycles. Red vertical lines indicate  $\log p_{\{k^{(0)}\}}$ , the log-probabilities of obtaining the**  
 81 **frequency distribution  $k^{(0)}$  from  $p_h$ .  $p$ -values are obtained by taking the quantile of the  $\log p_{\{k^{(0)}\}}$  within the 1,000,000 log-**  
 82 **probabilities of bootstrap samples.**

83

Number of  $R_{\text{phase}}$  extremes found at  $x$  hours from nearest tidal high water

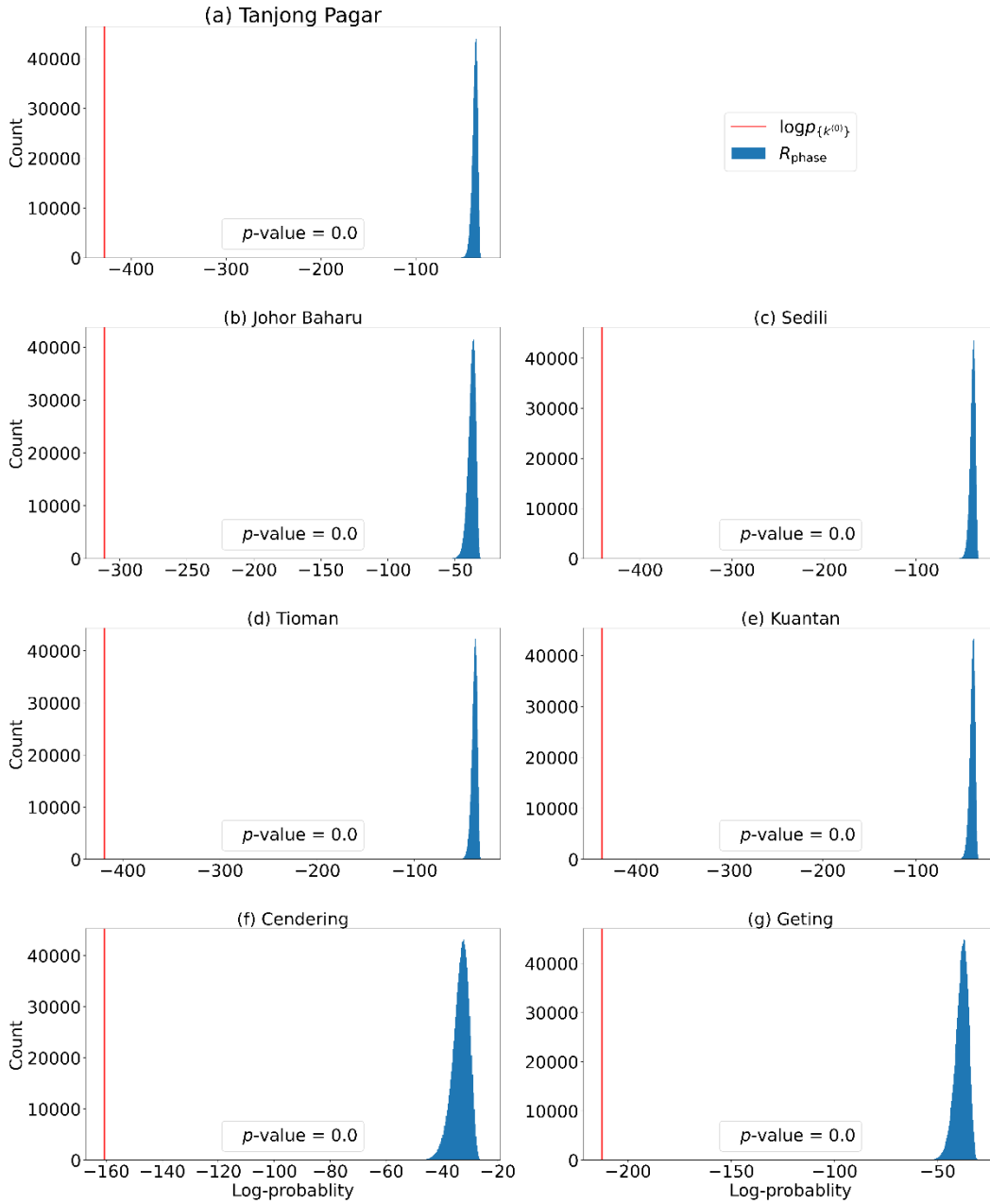


84

85 **Figure S13: The frequency distribution for extreme values of  $R_{\text{phase}}$  and the No-TSI distribution during semidiurnal tidal cycles,**  
 86 **truncated at  $\pm 8$  hours from tidal high water. The frequency distribution is compared to the No-TSI distribution to determine the**  
 87 **presence of tide-surge interaction. Summary statistics of the frequency distribution are shown using the horizontal notched box plot,**  
 88 **where orange lines indicate the medians, notches indicate the 95% confidence interval of the medians, notched rectangles indicate**  
 89 **the interquartile range (IQR), whiskers indicate a range that extends up to  $1.5 \times \text{IQR}$  from the limits of the IQR, and black circles (if**  
 90 **present) indicate outliers outside this range.**

91

Distribution of bootstrap sample log-probability



92

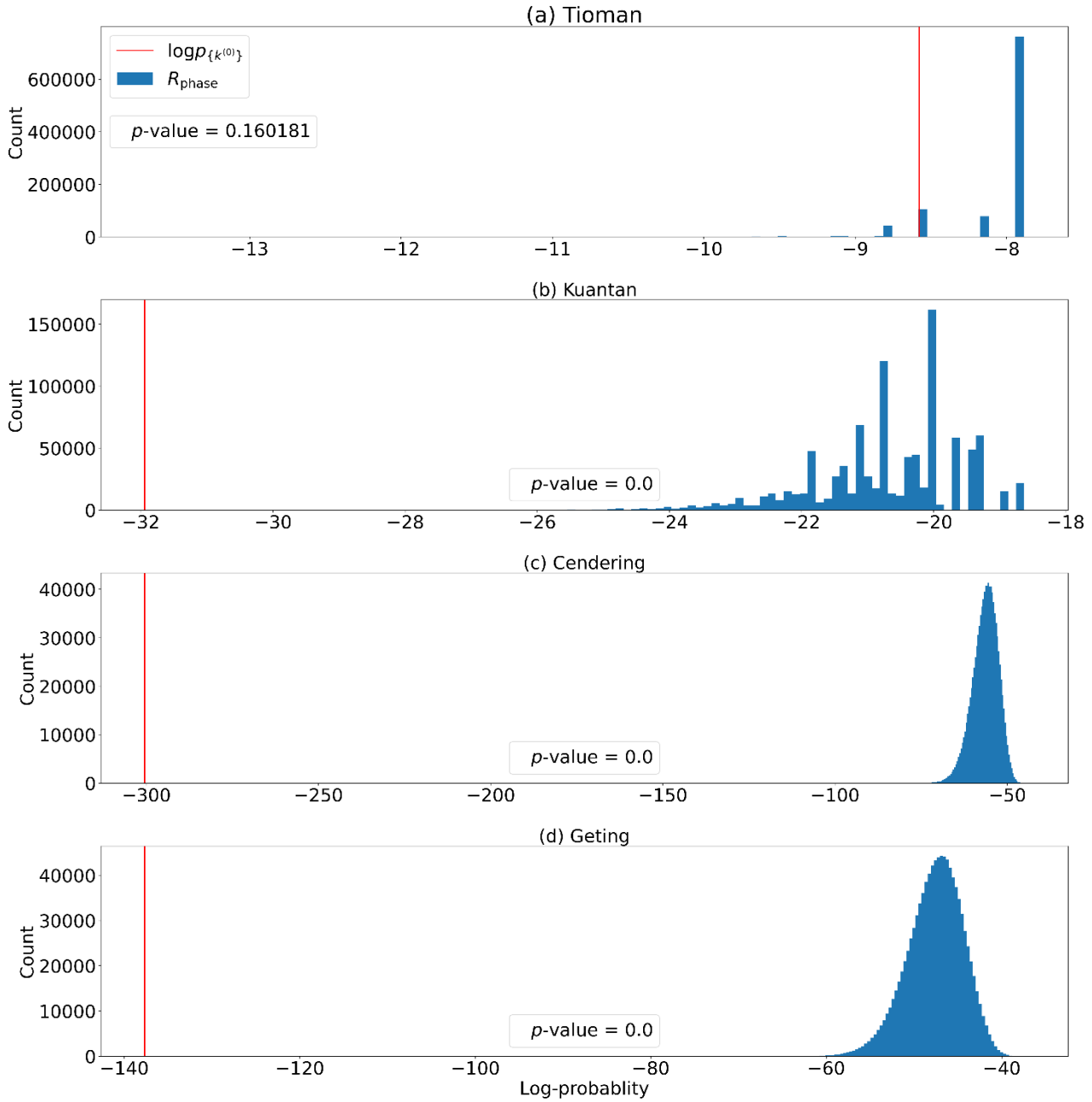
93 **Figure S14: Histogram of 1,000,000 log-probabilities of obtaining a randomly generated bootstrap sample from the normalized No-**  
 94 **TSI distribution  $p_h$  of  $R_{\text{phase}}$  during semidiurnal tidal cycles. Red vertical lines indicate  $\log p_{\{k^{(0)}\}}$ , the log-probabilities of obtaining**  
 95 **the frequency distribution  $k^{(0)}$  from  $p_h$ .  $p$ -values are obtained by taking the quantile of the  $\log p_{\{k^{(0)}\}}$  within the 1,000,000 log-**  
 96 **probabilities of bootstrap samples.**

97





Distribution of bootstrap sample log-probability

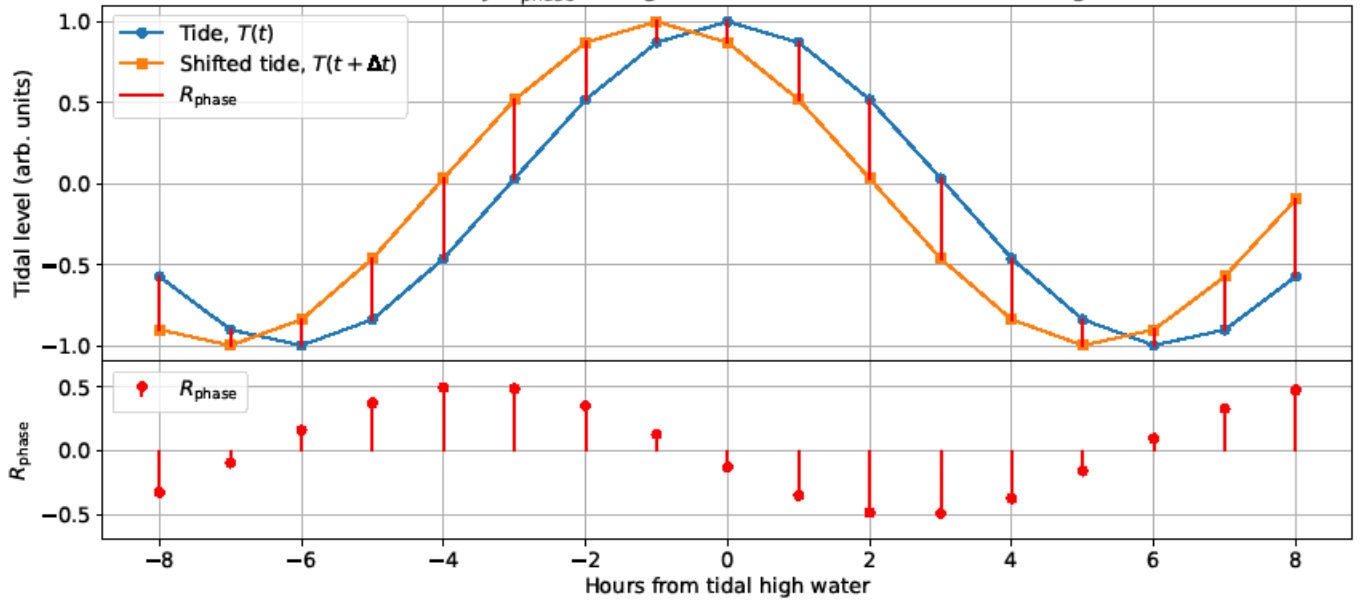


106

107 **Figure S16: Histogram of 1,000,000 log-probabilities of obtaining a randomly generated bootstrap sample from the normalized No-**  
 108 **TSI distribution  $p_h$  of  $R_{\text{phase}}$  during diurnal tidal cycles. Red vertical lines indicate  $\log p_{\{k^{(0)}\}}$ , the log-probabilities of obtaining the**  
 109 **frequency distribution  $k^{(0)}$  from  $p_h$ .  $p$ -values are obtained by taking the quantile of the  $\log p_{\{k^{(0)}\}}$  within the 1,000,000 log-**  
 110 **probabilities of bootstrap samples.**

111

Illustration of why  $R_{\text{phase}}$  is largest at 3 and 4 hours from tidal high water

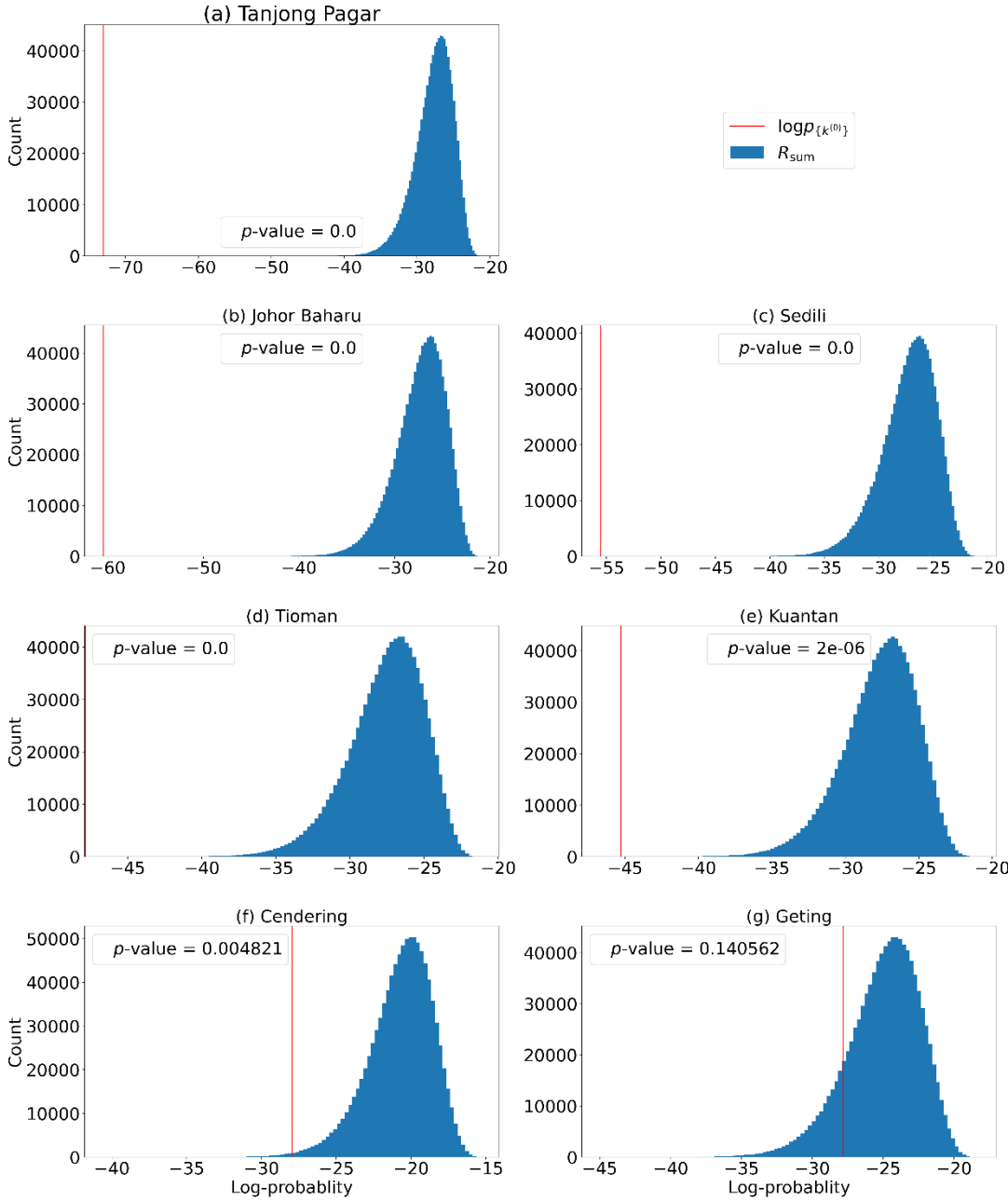


112

113 **Figure S17: The greatest vertical difference between two identical but slightly horizontally-displaced functions are near where the**  
114 **function has the steepest gradient. For semidiurnal tides, this corresponds to 3–4 hours from HW. Magnitude of the horizontal**  
115 **displacement is an arbitrary amount and exaggerated for the purpose of illustration.**

116

Distribution of bootstrap sample log-probability

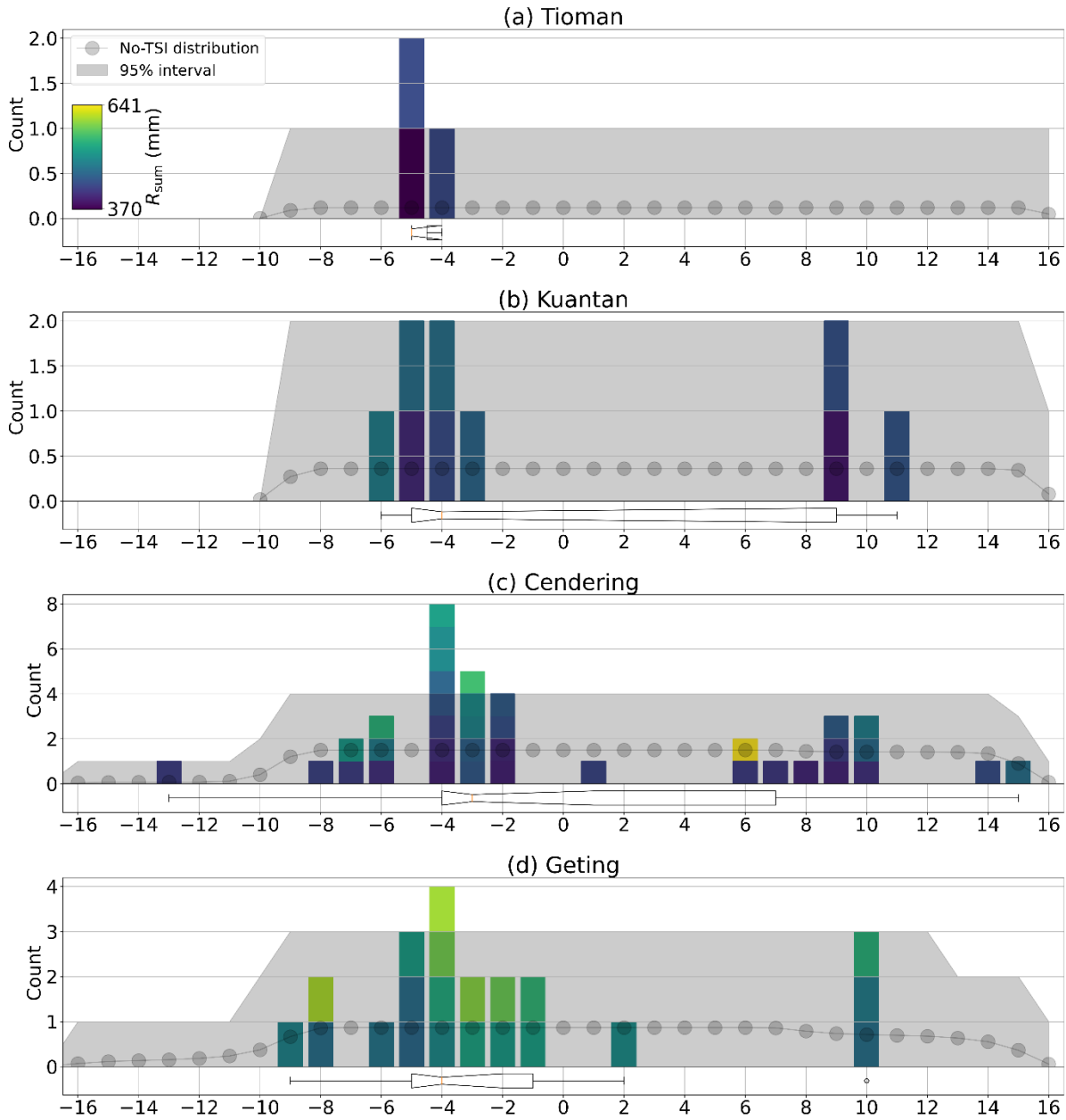


117

118 **Figure S18: Histogram of 1,000,000 log-probabilities of obtaining a randomly generated bootstrap sample from the normalized No-**  
 119 **TSI distribution  $p_h$  of  $R_{\text{sum}}$  during semidiurnal tidal cycles. Red vertical lines indicate  $\log p_{\{k^{(0)}\}}$ , the log-probabilities of obtaining**  
 120 **the frequency distribution  $k^{(0)}$  from  $p_h$ .  $p$ -values are obtained by taking the quantile of the  $\log p_{\{k^{(0)}\}}$  within the 1,000,000 log-**  
 121 **probabilities of bootstrap samples.**

122

Number of  $R_{sum}$  extremes found at x hours from nearest tidal high water

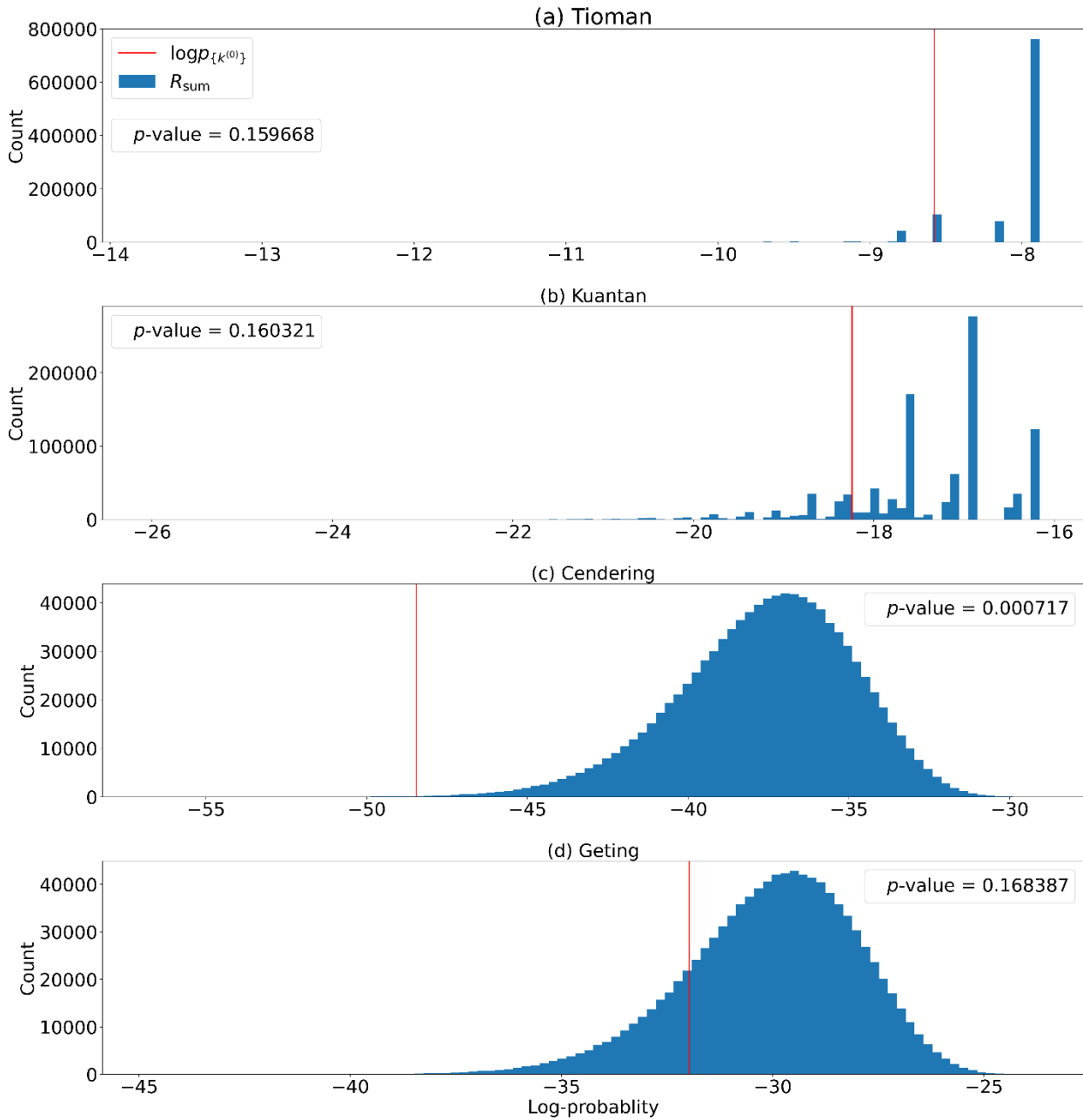


123

124 **Figure S19: The frequency distribution for extreme values of  $R_{sum}$  and the No-TSI distribution during diurnal tidal cycles, truncated**  
 125 **at  $\pm 16$  hours from tidal high water. The frequency distribution is compared to the No-TSI distribution to determine the presence**  
 126 **of tide-surge interaction. Summary statistics of the frequency distribution are shown using the horizontal notched box plot, where**  
 127 **orange lines indicate the medians, notches indicate the 95% confidence interval of the medians, notched rectangles indicate the**  
 128 **interquartile range (IQR), whiskers indicate a range that extends up to  $1.5 \times IQR$  from the limits of the IQR, and black circles (if**  
 129 **present) indicate outliers outside this range.**

130

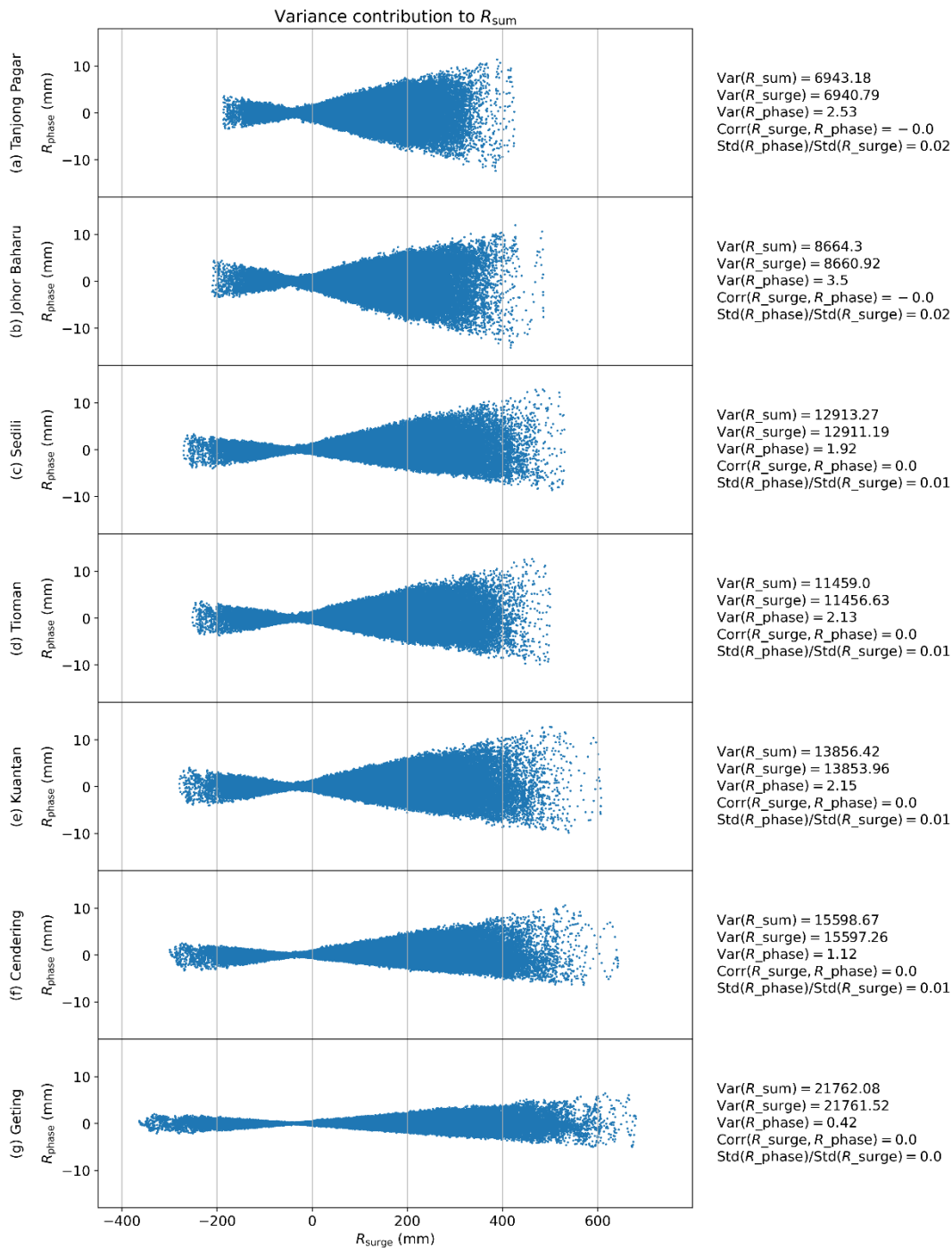
Distribution of bootstrap sample log-probability



131

132 **Figure S20: Histogram of 1,000,000 log-probabilities of obtaining a randomly generated bootstrap sample from the normalized No-**  
 133 **TSI distribution  $p_h$  of  $R_{\text{sum}}$  during diurnal tidal cycles. Red vertical lines indicate  $\log p_{\{k^{(0)}\}}$ , the log-probabilities of obtaining the**  
 134 **frequency distribution  $k^{(0)}$  from  $p_h$ .  $p$ -values are obtained by taking the quantile of the  $\log p_{\{k^{(0)}\}}$  within the 1,000,000 log-**  
 135 **probabilities of bootstrap samples.**

136



137

138 **Figure S21: Scatter plots between  $R_{wind}$  and  $R_{phase}$  at each tide gauge location and how they contribute to  $R_{sum}$ . Values of  $-0.0$  is**  
 139 **a small negative value between  $-0.05$  and  $0$ .**

140



141 **References**

142 Caldwell, P. C., Merrifield, M. A., and Thompson, P. R.: Sea level measured by tide gauges from global  
143 oceans as part of the Joint Archive for Sea Level (JASL) since 1846,  
144 <https://doi.org/10.7289/V5V40S7W>, 2001.

145 GEBCO Compilation Group: The GEBCO\_2023 Grid – a continuous terrain model of the global oceans  
146 and land, NERC EDS British Oceanographic Data Centre NOC [data set],  
147 <https://doi.org/10.5285/f98b053b-0cbc-6c23-e053-6c86abc0af7b>, 2023.

148 OpenStreetMap contributors: Planet dump retrieved from <https://planet.osm.org>,  
149 <https://www.openstreetmap.org>, accessed: 2024-04-30, 2017.

150